Thai Journal of Mathematics
Volume 13 (2015) Number 3 : 775–788
http://thaijmath.in.cmu.ac.th
ISSN 1686-0209

Numerical Treatment to a Water-Quality Measurement Model in an Opened-Closed Reservoir

Witsarut Kraychang[1] and Nopparat Pochai

Department of Mathematics, Faculty of Science
King Mongkut's Institute of Technology Ladkrabang
Bangkok 10520, Thailand
e-mail : Witsarut_popmath@hotmail.com (W. Kraychang)
Nop_math@yahoo.com (N. Pochai)

Centre of Excellence in Mathematics
Commission on Higher Education (CHE)
Si Ayutthaya Road, Bangkok 10400, Thailand

Abstract : Measuring the water quality in water sources or the Monkey Cheeks Project with opened-closed reservoir. It can be measured by the field measurement, using the water quality monitoring tools and the water quality models consist of hydrodynamic model and dispersion model, to calculate the quality of the water. Hydrodynamic model, using the shallow water equation as a governing equation, is used to describe the water current, having source of wave maker and bottom topography as the required data, bringing about the elevation and velocities of water. Dispersion model, using the advection-diffusion equation as the governing equation, is used to describe the spread of the pollutant concentration of water, having pollutant concentration at point source and calculated water velocities from the first model as the input data, bringing the time-dependent pollutant concentration of water at any point. In this research, the three-dimensional surface fitting technique is employed, the anisotropic bottom topography data is represented by a surface function in the hydrodynamic model, in order to have a more realistic water current and water quality approximations in opened-closed reservoir.

Keywords : water quality model; hydrodynamic model; dispersion model; advection-diffusion equation; opened-closed reservoir.
2010 Mathematics Subject Classification : 76R50; 39A14; 35Q30; 35L51.

[1]Corresponding author.

1 Introduction

There are many methods for detecting the level of pollutants in the water, mostly conducted by a field measurement and a mathematical simulation. The shallow water mass transport's problems are presented in [1], as the method of characteristics has been reported applied. In [2], [3] and [4], the finite element method for solving steady and unsteady water pollution measurements are introduced. The various numerical techniques of solving the uniform flow of stream water quality model are presented in [5], [6] and [7]. The numerical methods of approximating the solution of the two-dimensional advection-diffusion-reaction equation are proposed in [5], [8] and [9].

Most non-uniform flow models need the input data concerned with the velocity of the current at any point and any time in the domain. The hydrodynamic model provides the velocity field and the elevation of the water. In [10, 5, 8, 9, 6, 7], the hydrodynamic model and advection-diffusion equation are used to approximate the velocity of the water current in a bay and a channel. In [9] and [11], the results from hydrodynamic model are used as data for the non-uniform flow of the advection-diffusion-reaction equation, which provide the pollutant concentration field. The term of the friction forces occurred thanks to the drag of sides of the uniform reservoir. The theoretical solution of the model was found at the ending point of the domain and the analytical solution to check the accuracy of our approximate solution was used. In [9], the Lax-Wendroff method with stability analysis to solve the two-dimensional hydrodynamic model with a rectangular domain was proposed. In [12], develop mathematical models and numerical methods for approximating water flow directions and pollutant concentration level in Rama-nine reservoirs in opened with two parallel canals and assuming bottom topography of reservoir is flat. The Lax-Wendroff method is subsequently used in non-dimensional form of a shallow water equation to approximate the velocity of water and elevation of water, we use the forward difference in time and backward difference in space of advection diffusion equation. In [4] and [13], the Lax-Wendroff method for solving the dimensional form of shallow water equation in rectangular model and spherical model with Matlab program are proposed, respectively.

In this research, we begin with modifying a mathematical model, combining two existing mathematical models, a hydrodynamic model which is used to describe the water current in an opened-closed reservoir and a dispersion model which is used to describe the diffusion of the pollutant concentration of water in an opened-closed reservoir. This is to make the proposed model suitable for the reservoir. The shallow water equation of the hydrodynamic model is assumed by averaging the equation over the depth with anisotropic bottom topography, and discarding the term regarding the Coriolis force, surface wind effect and external forces, resulting in the calculated velocity used in the dispersion model to approximate the concentration levels of the pollutants.

2 Water-Quality Model

In this section, two mathematical models are described. They were used to simulate time-varying pollutant levels causing by wastewater discharges from external source into an opened-closed reservoir and drain water at the exit gate. The first model was a hydrodynamic model that determined the velocity and elevation of the water at any location in the reservoir with anisotropic bottom topography, while the second model was a pollutant dispersion model that determined the pollutant level at any point in the reservoir.

2.1 Hydrodynamic model: anisotropic bottom topography

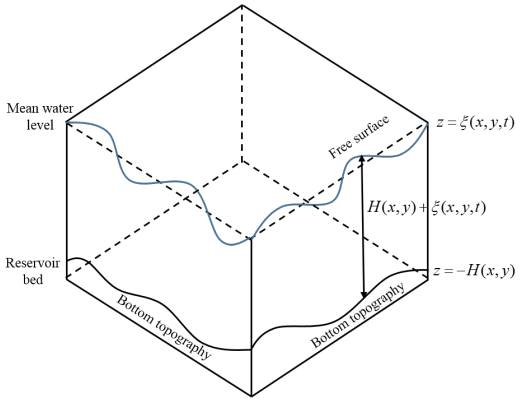

Figure 1: Cross-section of the reservoir.

The two-dimensional unsteady flow of water into and out of the reservoir could be determined by using the system of shallow water equations as the conservation of mass and conservation of momentum were taken into account. the equations of this system could be derived from depth-averaging the Navier-Stokes equations in the vertical direction, neglecting the diffusion of momentum due to turbulence and discarding the terms expressing the effects of friction, surface wind, Coriolis factor and shearing stresses. The continuity equation is then expressed as follows:

$$\frac{\partial h}{\partial t} + \frac{\partial (uh)}{\partial x} + \frac{\partial (vh)}{\partial y} = 0, \tag{2.1}$$

and the momentum equations are expressed as below:

$$\frac{\partial (uh)}{\partial t} + \frac{\partial (u^2 h + \frac{1}{2} g h^2)}{\partial x} + \frac{\partial (uvh)}{\partial y} = 0, \tag{2.2}$$

$$\frac{\partial (vh)}{\partial t} + \frac{\partial (uvh)}{\partial x} + \frac{\partial (v^2 h + \frac{1}{2} g h^2)}{\partial y} = 0, \tag{2.3}$$

where

$h(x,y,t)$ is the depth measured from the mean surface of water to the reservoir bed $h = H + \xi$ (m),

$\xi(x,y,t)$ is the elevation of surface of water from the mean water level in reservoir (sea level) (m),

$H(x,y)$ is the interpolated bottom topography function of the reservoir (m),

$u(x,y,t)$ is velocity in x direction (m/s),

$v(x,y,t)$ is velocity in y direction (m/s),

g is gravitational constant $(9.8m/s^2)$.

Such time (t), and two space coordinates, x and y are the independent variables. Likewise, the conserved quantities are mass, which is proportional to h, and momentum, which is proportional to (uh) and (vh). As taken with respect to the same term, the partial derivatives are grouped into vectors $(\partial x, \partial y.\partial t)$ and later rewritten as a hyperbolic partial differential equation as follows:

$$U = \begin{pmatrix} h \\ uh \\ vh \end{pmatrix}, F(U) = \begin{pmatrix} uh \\ u^2h + \frac{1}{2}gh^2 \\ uvh \end{pmatrix}, G(U) = \begin{pmatrix} vh \\ uvh \\ v^2h + \frac{1}{2}gh^2 \end{pmatrix}. \quad (2.4)$$

The hyperbolic PDE:

$$\frac{\partial U}{\partial t} + \frac{\partial}{\partial t}F(U) + \frac{\partial}{\partial t}G(U) = 0. \quad (2.5)$$

The initial conditions of reservoir were as follows: the x and y-velocity components

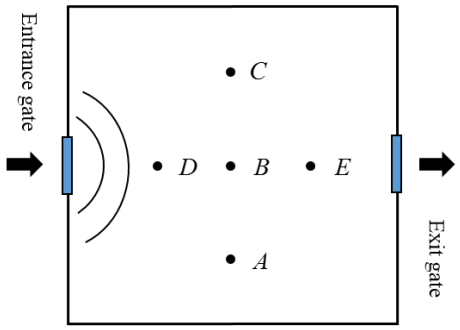

Figure 2: Opened-closed reservoir and observation points A, B, C, D and E

were zero as well as the water elevation: $u = 0, v = 0$ and $\xi = 0$, while the boundary conditions were as follows: (i) $\frac{\partial u}{\partial x} = 0$, $\frac{\partial v}{\partial y} = 0$, $\xi = 0$ for the horizontal edges of the rectangular reservoir; (ii) $\frac{\partial u}{\partial x} = 0$, $v = 0$, $\xi = 0$ for the vertical edges; and (iii) $\xi = f(x,y)$ for the water flowing into the entrance gate and $\frac{\partial u}{\partial x} = u_1$, $\frac{\partial v}{\partial y} = 0$ for the velocity of water flow at exit gate as shown in Figure.2.

2.2 Dispersion model

When applying the distributed pollutant process, including the transportation and diffusion, the mass transfer equation is satisfied by averaging the equation over the depth, generating the advection-diffusion equation,

$$\frac{\partial C}{\partial t} + u\frac{\partial C}{\partial x} + v\frac{\partial C}{\partial y} = D\left(\frac{\partial^2 C}{\partial x^2} + \frac{\partial^2 C}{\partial y^2}\right), \tag{2.6}$$

where $C(x, y, t)$ (kg/m^3) is the concentration averaged in depth at the displacement (x, y) and at time t , $D(m^2/s)$ is the diffusion coefficient.

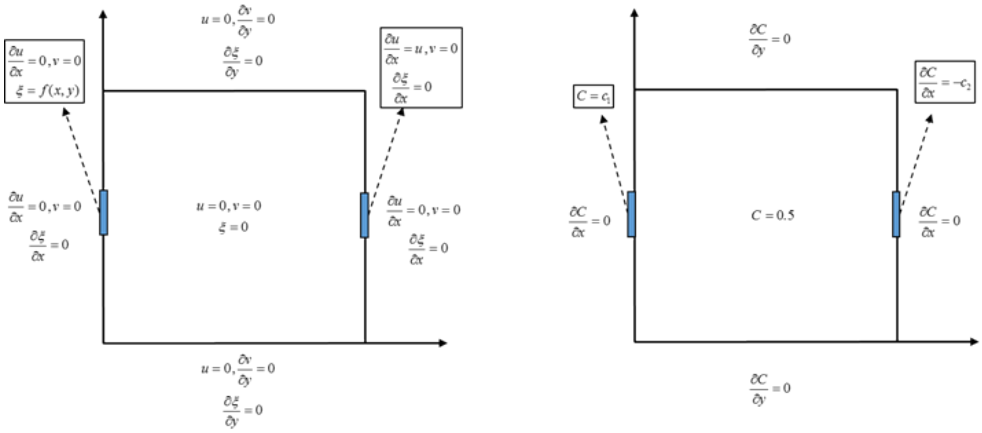

Figure 3: Initial condition and boundary condition of hydrodynamic model and dispersion model.

The water pollutant was discharged from the entrance gate into the opened-closed reservoir by assuming the pollutant concentration constant as function c_- and this reservoir had draining water at the exit gate by assuming rate of drain of water as $\frac{\partial C}{\partial x} = -c_2$. Initial pollutant concentration in reservoir was $0.5(kg/m^3)$ and there was no rate of change of pollutant concentration at the boundary of reservoir as Figure.3.

3 Numerical Technique

3.1 Numerical method for the hydrodynamic model

We would use the Lax-Wendroff method to compute a numerical approximation to the solution of hyperbolic PDE (2.5). A regular square finite difference grid with a vector-valued solution centred in the grid cells. The domain of problem $L \times M$ dimension, l and m were subintervals, such that $l\Delta x = L$, $m\Delta y = M$ and interval time $[0, T]$, k was subintervals, such that $k\Delta t = T$,$U^n_{i,j} = U(x, y, t)$

represents a three component vector at each cell i, j with time step n , where $x = i\Delta x$, $y = j\Delta y$ and $t = k\Delta t$.
Step 1: Compute initial vector $U^n_{i,j}$ at centre cells.

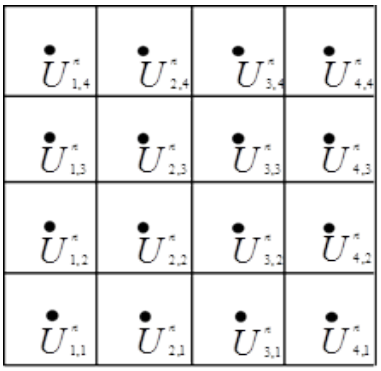

Figure 4: At the beginning of a time step, the variables represent the solution at the centres of the grids.

Step 2: Take $U^n_{i,j}$ to compute vector $F^n_{i,j}$ and $G^n_{i,j}$ at centre cells.

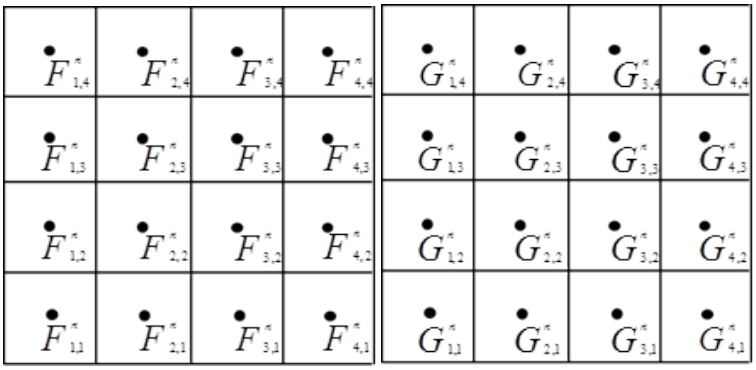

(a) (b)

Figure 5: The vector (a) F at centres of grid (b) G at centres of grid.

Step 3: This stage is a half-step; it defines values of U at time step $n + \frac{1}{2}$ and the midpoints of the edges of the grid.

$$U^{n+\frac{1}{2}}_{i+\frac{1}{2},j} = \frac{1}{2}(U^n_{i+1,j} + U^n_{i,j}) - \frac{\Delta t}{2\Delta x}(F^n_{i+1,j} - F^n_{i,j}) \tag{3.1}$$

$$U^{n+\frac{1}{2}}_{i,j+\frac{1}{2}} = \frac{1}{2}(U^n_{i,j+1} + U^n_{i,j}) - \frac{\Delta t}{2\Delta y}(G^n_{i,j+1} - G^n_{i,j}) \tag{3.2}$$

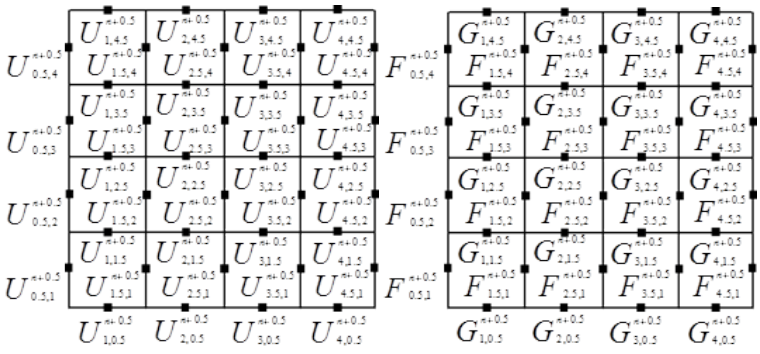

(a) (b)

Figure 6: The values of vector (a) U represent the solution at the midpoints of the grids and (b) F, G at the midpoints of the grids.

Step 4: Take values of U from step 3 to compute F, G at time step $n + \frac{1}{2}$ and the midpoints of the edges of the grid.
Step 5: The last step completes the time step by using the values computed in the step 1 and step 4 to compute new values at the centres of the cells.

$$U_{i,j}^{n+1} = U_{i,j}^{n} - \frac{\Delta t}{\Delta x}(F_{i+\frac{1}{2},j}^{n+\frac{1}{2}} - F_{i-\frac{1}{2},j}^{n+\frac{1}{2}}) - \frac{\Delta t}{\Delta y}(G_{i,j+\frac{1}{2}}^{n+\frac{1}{2}} - G_{i,j-\frac{1}{2}}^{n+\frac{1}{2}}) \tag{3.3}$$

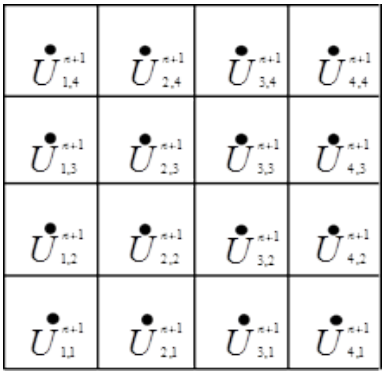

Figure 7: The solution U^{n+1} at centres of the grids.

We would use the finite difference method to compute a numerical approximation to the boundary conditions of the reservoir.
For left boundary condition, where $i = 0$ and $1 \leqslant j \leqslant m$, therefore $U_{0,j}^{n} = U_{1,j}^{n}$, substituting the approximate unknown vector nodes $U_{0,j}^{n}$ of left boundary into

(3.1), we had

$$U^{n+\frac{1}{2}}_{\frac{1}{2},j} = \frac{1}{2}(U^n_{1,j} + U^n_{0,j}) - \frac{\Delta t}{2\Delta x}(F^n_{1,j} - F^n_{0,j}) = U^n_{1,j} \tag{3.4}$$

For right boundary condition, where $i = l$ and $1 \leqslant j \leqslant m$, therefore $U^n_{l+1,j} = U^n_{l,j}$, substituting the approximate unknown vector nodes $U^n_{i+1,j}$ of right boundary into (3.1), we had

$$U^{n+\frac{1}{2}}_{l+\frac{1}{2},j} = \frac{1}{2}(U^n_{l+1,j} + U^n_{l,j}) - \frac{\Delta t}{2\Delta x}(F^n_{l+1,j} - F^n_{l,j}) = U^n_{l,j} \tag{3.5}$$

For lower boundary condition, where $1 \leqslant i \leqslant l$ and $j = 0$, therefore $U^n_{i,0} = U^n_{i,1}$, substituting the approximate unknown vector nodes $U^n_{i,0}$ of lower boundary into (3.2), we had

$$U^{n+\frac{1}{2}}_{i,\frac{1}{2}} = \frac{1}{2}(U^n_{i,1} + U^n_{i,0}) - \frac{\Delta t}{2\Delta y}(G^n_{i,1} - G^n_{i,0}) = U^n_{i,1} \tag{3.6}$$

For upper boundary condition, where $1 \leqslant i \leqslant l$ and $j = m$, therefore $U^n_{i,m+1} = U^n_{i,m}$, substituting the approximate unknown vector nodes $U^n_{i,0}$ of upper boundary into (3.2), we had

$$U^{n+\frac{1}{2}}_{i,m+\frac{1}{2}} = \frac{1}{2}(U^n_{i,m+1} + U^n_{i,m}) - \frac{\Delta t}{2\Delta y}(G^n_{i,m+1} - G^n_{i,0}) = U^n_{i,m} \tag{3.7}$$

3.2 Numerical method for the dispersion model

We used the forward differences in time and backward difference in space in advection-diffusion equation. We can approximate $C^n_{i,j}$, the value of the approximation of $C(x, y, t)$ at point $x = i\Delta x$, $y = j\Delta y$ and $t = n\Delta t$, where $1 \leq i \leq l$, $1 \leq j \leq m$ and $0 \leq n \leq k$.

$$\frac{\partial C}{\partial t} = \frac{C^{n+1}_{i,j} - C^n_{i,j}}{\Delta t}, \tag{3.8}$$

$$\frac{\partial C}{\partial x} = \frac{C^n_{i,j} - C^n_{i-1,j}}{\Delta x}, \tag{3.9}$$

$$\frac{\partial C}{\partial y} = \frac{C^n_{i,j} - C^n_{i,j-1}}{\Delta y}, \tag{3.10}$$

$$\frac{\partial^2 C}{\partial x^2} = \frac{C^n_{i+1,j} - 2C^n_{i,j} + C^n_{i-1,j}}{(\Delta x)^2}, \tag{3.11}$$

$$\frac{\partial^2 C}{\partial y^2} = \frac{C^n_{i,j+1} - 2C^n_{i,j} + C^n_{i,j-1}}{(\Delta y)^2}. \tag{3.12}$$

Taking the forward in time and backward in space (2.6), we got the following finite difference equation,

$$\frac{C_{i,j}^{n+1}-C_{i,j}^{n}}{\Delta t}+u_{i,j}^{n}\left(\frac{C_{i,j}^{n}-C_{i-1,j}^{n}}{\Delta x}\right)+v_{i,j}^{n}\left(\frac{C_{i,j}^{n}-C_{i,j-1}^{n}}{\Delta y}\right)=,$$
$$D\left(\frac{C_{i+1,j}^{n}-2C_{i,j}^{n}+C_{i-1,j}^{n}}{(\Delta x)^{2}}+\frac{C_{i,j+1}^{n}-2C_{i,j}^{n}+C_{i,j-1}^{n}}{(\Delta y)^{2}}\right) \tag{3.13}$$

$$C_{i,j}^{n+1}=\frac{\Delta tD}{\Delta x^{2}}C_{i+1,j}^{n}+\frac{\Delta tD}{\Delta y^{2}}C_{i,j+1}^{n}+\left(\frac{\Delta t}{\Delta x}u_{i,j}^{n}+\frac{\Delta t}{\Delta x^{2}}D\right)C_{i-1,j}^{n}+$$
$$\left(\frac{\Delta t}{\Delta y}v_{i,j}^{n}+\frac{\Delta t}{\Delta y^{2}}D\right)C_{i,j-1}^{n}+\left(1-\frac{\Delta t}{\Delta x}u_{i,j}^{n}-\frac{\Delta t}{\Delta y}v_{i,j}^{n}-\frac{2D\Delta t}{\Delta x^{2}}-\frac{2D\Delta t}{\Delta y^{2}}\right)C_{i,j}^{n}, \tag{3.14}$$

where D was the diffusion coefficient (m^2/s).

If $C_{i,j}^{n}$ lay at the boundary of the opened-closed reservoir, it was calculated by applying the backward difference scheme at right boundary and top boundary, forward difference scheme at left boundary and bottom boundary. For left boundary condition, where $i=1$ and $1\leq j\leq m$, therefore $C_{0,j}^{n}=C_{1,j}^{n}$, substituting the approximate unknown vector nodes $C_{0,j}^{n}$ of left boundary into (3.13), we had

$$\frac{C_{1,j}^{n+1}-C_{1,j}^{n}}{\Delta t}+v_{1,j}^{n}\left(\frac{C_{1,j}^{n}-C_{1,j-1}^{n}}{\Delta y}\right)=$$
$$D\left(\frac{C_{2,j}^{n}-C_{1,j}^{n}}{(\Delta x)^{2}}+\frac{C_{1,j+1}^{n}-2C_{1,j}^{n}+C_{1,j-1}^{n}}{(\Delta y)^{2}}\right), \tag{3.15}$$

For right boundary condition, where $i=l$ and $1\leq j\leq m$, therefore $C_{i+1,j}^{n}=C_{1,j}^{n}$, substituting the approximate unknown vector nodes $C_{i+1,j}^{n}$ of right boundary into (3.13), we had

$$\frac{C_{l,j}^{n+1}-C_{l,j}^{n}}{\Delta t}+u_{l,j}^{n}\left(\frac{C_{l,j}^{n}-C_{l-1,j}^{n}}{\Delta x}\right)+v_{l,j}^{n}\left(\frac{C_{l,j}^{n}-C_{l,j-1}^{n}}{\Delta y}\right)$$
$$=D\left(\frac{-C_{l,j}^{n}+C_{l-1,j}^{n}}{(\Delta x)^{2}}+\frac{C_{l,j+1}^{n}-2C_{l,j}^{n}+C_{l,j-1}^{n}}{(\Delta y)^{2}}\right), \tag{3.16}$$

For lower boundary condition, where $1\leq i\leq l$ and $j=1$, therefore $C_{i,0}^{n}=C_{i,1}^{n}$, substituting the approximate unknown vector nodes $C_{0,j}^{n}$ of lower boundary into (3.13), we had

$$\frac{C_{i,1}^{n+1}-C_{i,1}^{n}}{\Delta t}+u_{i,1}^{n}\left(\frac{C_{i,1}^{n}-C_{i-1,1}^{n}}{\Delta x}\right)$$
$$=D\left(\frac{C_{i+1,1}^{n}-2C_{i,1}^{n}+C_{i-1,1}^{n}}{(\Delta x)^{2}}+\frac{C_{i,2}^{n}-C_{i,1}^{n}}{(\Delta y)^{2}}\right), \tag{3.17}$$

For upper boundary condition, where $1 \leq i \leq l$ and $j = m$, therefore $C^n_{i,m+1} = C^n_{i,m}$, substituting the approximate unknown vector nodes $C^n_{i,m+1}$ of left boundary into (3.13), we had

$$\frac{C^{n+1}_{i,m} - C^n_{i,m}}{\Delta t} + u^n_{i,m}\left(\frac{C^n_{i,m} - C^n_{i-1,m}}{\Delta x}\right) + v^n_{i,m}\left(\frac{C^n_{i,m} - C^n_{i,m-1}}{\Delta y}\right)$$
$$= D\left(\frac{C^n_{i+1,m} - 2C^n_{i,m} + C^n_{i-1,m}}{(\Delta x)^2} + \frac{-C^n_{i,m} + C^n_{i,m-1}}{(\Delta y)^2}\right), \tag{3.18}$$

4 Numerical Experiments

In this section, various results were reported in a table, several surface and contour plots, and a comparison graph. Hydrodynamic model, calculated the velocities of water and elevation of water in opened-closed reservoir with an empirical anisotropic bottom topography interpolated function $0.01sin(0.01(x+y))$ as shown in Figure.8, using Lax-Wendroff method, when water flowed into the entrance gate by using the elevation of water $\xi = 1(m)$ and discarding drain water though the exit gate, using the rate of change of velocity u at $0.5(m/s^2)$, the results as shown in Figure.9 and Figure.10 for time $0sec$ to $50sec$. Dispersion model, calculated the pollutant concentration of water in opened-closed reservoir by using finite difference method, when wastewater was discharged from the external source into the reservoir and drain water was released thru the exit gate by using the rate of change of pollutant concentration with respect to x-coordinate at $0.1(kg/m^4)$ with initial pollutant concentration in this reservoir at $0.02(kg/m^3)$.

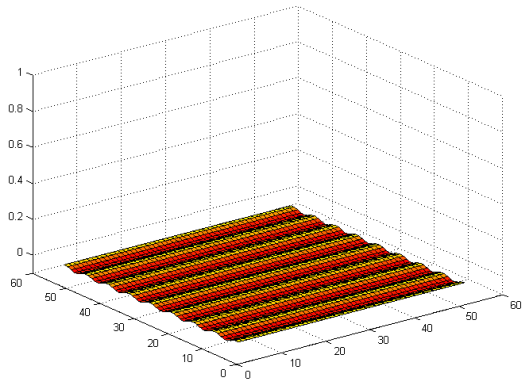

Figure 8: Anisotropic bottom topography surface in the opened-close reservoir

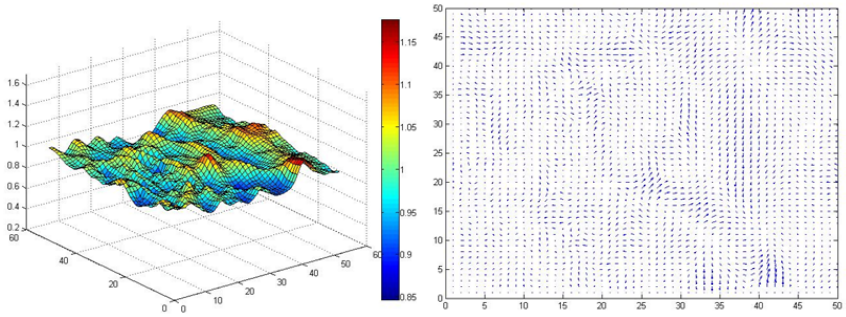

(a) (b)

Figure 9: Time 50 sec, (a) surface plot of elevation of water (b) vector field of velocities in opened-closed reservoir.

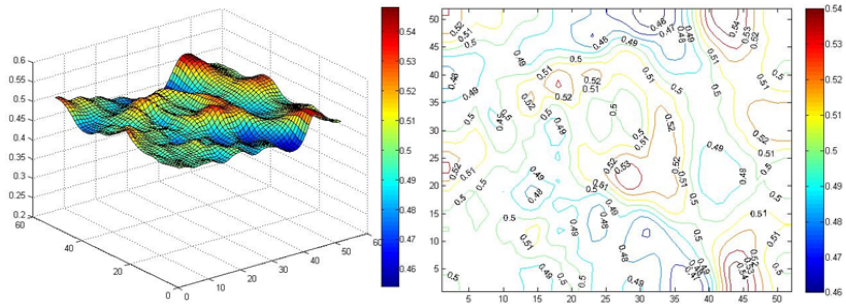

(a) (b)

Figure 10: Time 50 sec, (a) surface plot (b) contour plot of pollutant concentration in opened-closed reservoir.

The monitoring points in opened-closed reservoir was used to observe the dispersion of pollutant concentration of water. In Figure.11(a) showing the comparison of pollutant concentration at monitoring point A, B and C and Figure.11(b) showing the comparison of pollutant concentration at monitoring point D and E for time $0sec$ to $50sec$.

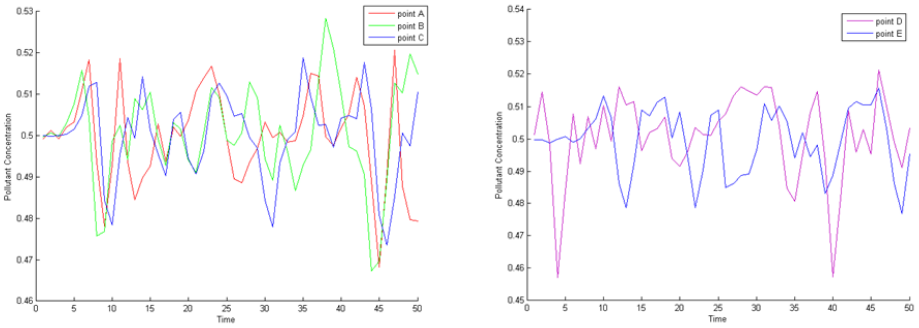

(a) (b)

Figure 11: The comparison of pollutant concentration at monitoring (a) of point A, B and C and monitoring (b) of point D and E.

The pollutant concentration of water at monitoring point A, B, C, D and E in the opened-closed reservoir was observed in every $25sec$ for time $0sec$ to $200sec$ with wastewater discharging from the external source every $36sec$ into reservoir and drain water releasing though the exit gate every $36sec$ in Table.1, wastewater discharging from the external source every $36sec$ into reservoir and drain water releasing though the exit gate every $72sec$ in Table.2 and wastewater discharging from external source every $72sec$ into reservoir and drain water releasing though the exit gate every $36sec$ in Table.3.

Table 1: Pollutant Concentration (kg/m^3) at observation points in reservoir case 1.

Point\Time (sec)	25	50	75	100	125	150	175	200
A	0.4988	0.4794	0.4967	0.4973	0.5122	0.5187	0.4577	0.5291
B	0.4988	0.5148	0.5053	0.5177	0.4741	0.5029	0.4824	0.5098
C	0.5095	0.5106	0.4924	0.5015	0.4937	0.5508	0.4635	0.4929
D	0.5055	0.5032	0.4913	0.5083	0.5205	0.4926	0.5158	0.5115
E	0.5089	0.4953	0.5021	0.4628	0.5040	0.5078	0.5608	0.4713

Table 2: Pollutant Concentration (kg/m^3) at observation points in reservoir case 2.

Point\Time (sec)	25	50	75	100	125	150	175	200
A	0.4988	0.4796	0.4969	0.4976	0.5126	0.5191	0.4581	0.5298
B	0.4988	0.5150	0.5055	0.5179	0.4745	0.5034	0.4828	0.5106
C	0.5095	0.5107	0.4926	0.5017	0.4940	0.5513	0.4640	0.4936
D	0.5055	0.5032	0.4915	0.5085	0.5208	0.4930	0.5163	0.5121
E	0.5089	0.4957	0.5024	0.4630	0.5047	0.5084	0.5613	0.4721

Table 3: Pollutant Concentration (kg/m^3) at observation points in reservoir case 3.

Point\Time (sec)	25	50	75	100	125	150	175	200
A	0.4988	0.4855	0.4979	0.4982	0.5062	0.5150	0.4863	0.4968
B	0.4988	0.5084	0.4889	0.5196	0.4785	0.5247	0.4690	0.5296
C	0.5095	0.4953	0.4882	0.5073	0.4932	0.5377	0.4628	0.5097
D	0.5055	0.4911	0.4913	0.5189	0.5238	0.4882	0.5013	0.5221
E	0.5089	0.5067	0.5143	0.4597	0.4947	0.4921	0.5434	0.4835

5 Discussion and Conclusion

In this research, a mathematical model to calculate the elevation of water, water current and pollutant concentration of water in opened-closed reservoir with anisotropic bottom topography at any point and any time, anisotropic bottom topography function could be interpolated from data of reservoir bed coordinate, using cubic spline interpolate technique. When compared to other points, monitoring point B at the center of opened-closed reservoir mostly had a high pollutant concentration, monitoring point D, near the entrance gate of reservoir, has a mostly lower pollutant concentration as shown in Figure.11.

To conclude the numerical simulation for water-quality measurement model in an opened-closed reservoir with an empirical anisotropic bottom topography was proposed and thus the mathematical models could calculate the elevation, the velocities and the pollutant concentration of water. The very models could adjust the bottom topography according to the varying reservoir bed, simulate the wave maker function at the entrance gate of reservoir from field data by using the data interpolation in order to have a more realistic water current and water quality approximations in opened-closed reservoir with anisotropic bottom topography.

Acknowledgement : The authors would like to thank the reviewers for their careful reading and constructive comments. The authors would like to also thank the "Centre of Excellence in Mathematics Program of the Commission on Higher Education" for support this research.

References

[1] A. Garzon, L. D'Alpaos, A modified method of the characteristic technique combined with Gelerkin finite element method to solve shallow water mass transport problems, Proceedings 23rd International Conference in Coastal Engineering 3 (1992) 3068-3080.

[2] P. Tabuenca, J. Vila, J. Cardona, A. Samartin, Finite element simulation of dispersion in the bay of Santander, Advanced in Engineering Software 28 (1997) 313-332.

[3] P. Tabuenca, J. Cardona, Numerical model for the study of hydrodynamics on bays and estuaries. Applied Mathematical Modeling 16 (1992) 78-85.

[4] C. Moler, Experiments with MATLAB, MathWorks 2015.

[5] N. Pochai, A numerical computation of a non-dimensional form of stream water quality model with hydrodynamic advection-dispersion-reaction equations, Journal of nonlinear analysis: hybrid systems 3 (2009) 666-673.

[6] N. Pochai, A numerical treatment of non-dimensional form of water quality model in a non-uniform flow stream using Saulyev scheme, Mathematical Problems in Engineering 2011 (2011) 491-317.

[7] N. Pochai, Numerical treatment of a modified MacCormack scheme in a nondimensional form of the water quality models in a nonuniform flow stream, Journal of Applied Mathematics 2014 (2014) 274-263.

[8] N. Pochai, C. Sornsiri, A non-dimensional form of hydrodynamic model with variable coefficients in a uniform reservoir using Lax-Wendroff method, Procedia Engineering 8 (2011) 89-93.

[9] N. Pochai, S. Tangmanee, L. J. Crane, J. J. H. Miller, A water quality computation in the uniform reservoir, Journal of Interdisciplinary Mathematics 12 (2009) 19-28.

[10] N. Pochai, A numerical computation of the non-dimensional form of a nonlinear hydrodynamic model in a uniform reservoir, Journal of nonlinear analysis: Hybrid systems 3 (2009) 463-466.

[11] N. Pochai, S. Tangmanee, L. J. Crane, J. J. H. Miller, A Finite Element Simulation of Water Quality Measurement in the Open Reservoir, Thai Journal of Mathematics 7 (2009) 77-93.

[12] W. Kraychang, N. Pochai, A Numerical Treatment of a Non-Dimensional From of a Water Quality Model in the Rama-nine Reservoir, Journal of Interdisplinary Mathematics 18 (2015) 375-394.

[13] C. R. Robinson, Shallow Water Equations, Syracuse University, 2011.

(Received 1 July 2015)
(Accepted 15 October 2015)